

# Luminescent Photoelectrochemical Cells. 5. Multiple Emission from Tellurium-Doped Cadmium Sulfide Photoelectrodes and Implications Regarding Excited-State Communication<sup>1</sup>

Bradley R. Karas, Holger H. Streckert, Rodney Schreiner, and Arthur B. Ellis\*

Contribution from the Chemistry Department, University of Wisconsin—Madison, Madison, Wisconsin 53706. Received October 24, 1980

**Abstract:** Samples of single-crystal, n-type, 100-ppm Te-doped CdS (CdS:Te) exhibit two emission bands when excited at several ultraband gap wavelengths. One emission band with  $\lambda_{\max} \approx 510$  nm is near the band gap of CdS:Te ( $\sim 2.4$  eV) and is likely edge emission. Its decay time, measured for samples immersed in sulfide solution (1 M OH<sup>-</sup>/1 M S<sup>2-</sup>) between 295 and 333 K, is faster than the pulse from the N<sub>2</sub>-pumped dye laser ( $\sim 7$  ns) used for 458-nm excitation. The other emissive transition,  $\lambda_{\max} \approx 600$  nm, involves intraband gap states introduced by Te. Intensity-time curves for this band have rise times of  $< 10$  ns and generally exhibit nonexponential decay; values of  $\tau_{1/2}$  are typically  $120 \pm 40$  and  $80 \pm 30$  ns at 295 and 333 K, respectively. When CdS:Te is used as the photoanode in a photoelectrochemical cell employing sulfide electrolyte, both emission bands are quenched in parallel during the passage of photocurrent resulting from 457.9- or 476.5-nm Ar ion laser excitation. Parallel quenching is observed at several temperatures for which the excited-state kinetic schemes are demonstrably different: open-circuit emission spectra reveal that both the absolute and relative intensities of the two emission bands are affected by temperature. With increasing temperature (295–333 K), the absolute intensities of both bands decline; a semilog plot of the ratio of 510- to 600-nm intensity vs.  $T^{-1}$  is linear with a slope corresponding to  $\sim 0.2$  eV, the energy gap between the two excited states. The existence of excited-state communication is inferred from the effects of temperature and electrode potential on multiple emission. Schemes for communication which are compatible with these results are discussed.

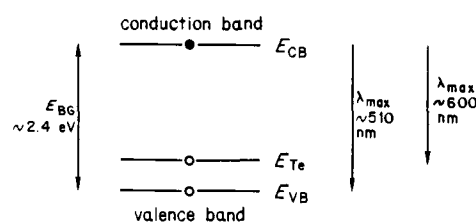
We recently reported that the emissive properties of n-type, tellurium-doped CdS (CdS:Te) electrodes can be used to probe electron-hole (e<sup>-</sup>-h<sup>+</sup>) pair recombination processes in photoelectrochemical cells (PECs).<sup>2</sup> In particular, emission intensity was found to be dependent on excitation wavelength and intensity, temperature, and electrode potential in a manner consistent with the photoelectrochemical band bending model.<sup>3</sup> A single emission band of subband gap energy was monitored in these studies ( $\lambda_{\max} \approx 600$  nm; the band gap,  $E_{\text{BG}}$ , of CdS:Te at low [Te] is believed<sup>4</sup> to be similar to that of undoped CdS,  $\sim 2.4$  eV<sup>5</sup> for which  $\lambda \approx 520$  nm).

While examining electroluminescence from CdS:Te, we saw, in addition to the 600-nm band, a second emission band of approximately band gap energy; both bands could also be observed in photoluminescence experiments under some conditions.<sup>6</sup> In this paper we utilize the energetic and kinetic features of multiple emission to construct a more detailed picture of the CdS:Te excited-state manifold and decay processes. In particular, by examining the effects of temperature and electrode potential on multiple emission, we demonstrate that excited-state communication may be inferred and characterized from PEC experiments.

## Results and Discussion

The samples of single-crystal, n-type, 100-ppm CdS:Te employed in this study exhibited two emission bands when excited at several ultraband gap wavelengths. Multiple emission was visibly apparent when the samples were excited at 337 nm with an intense, N<sub>2</sub> laser pulse: surface-localized green emission was

Scheme I



evident at the site of irradiation in addition to the global orange emission previously reported.<sup>2a</sup> The discrepancy in spatial distribution likely stems from the considerably greater absorptivity of CdS:Te for green light.

In sections below we discuss the spectral distribution and origin of the two emission bands, their decay times, and the effects of temperature upon emissive properties. The influence of electrode potential on multiple emission is characterized by using CdS:Te-based PECs. The final section of the paper is devoted to a description of several excited-state decay schemes which are consistent with our data.

**1. Spectral Distribution and Origin of Luminescence.** The 295-K, uncorrected, front-surface emission spectrum of single-crystal, n-type, 100-ppm CdS:Te is shown in curve 1 of Figure 1a. Two distinct emission bands—one sharp with  $\lambda_{\max} \approx 510$  nm, the other broad with  $\lambda_{\max} \approx 600$  nm—are observed for the dry crystal or, as displayed here, out of circuit in transparent sulfide (1 M OH<sup>-</sup>/1 M S<sup>2-</sup>) electrolyte. The 457.9-nm line of an Ar ion laser is the excitation source.

Both 100-ppm CdS:Te and nominally undoped CdS samples exhibit the 510-nm band, whose energy falls near the 2.4-eV band gap of CdS. Given its energy, sharpness, short lifetime (vide infra), and literature precedent,<sup>7</sup> this band is most likely edge emission in both CdS and CdS:Te. Additional support for such an assignment comes from the observed blue shift of  $\lambda_{\max}$  for this band to  $\sim 490$  nm at 77 K. This shift is in reasonable accord with the

(1) Parts 3 and 4 of this series are ref 2c and 6, respectively.  
 (2) (a) Karas, B. R.; Ellis, A. B. *J. Am. Chem. Soc.* **1980**, *102*, 968. (b) Ellis, A. B.; Karas, B. R. *Adv. Chem. Ser.* **1980**, No. 184, 185. (c) Karas, B. R.; Morano, D. J.; Bilich, D. K.; Ellis, A. B. *J. Electrochem. Soc.* **1980**, *127*, 1144.  
 (3) Gerischer, H. *J. Electroanal. Chem. Interfacial Electrochem.* **1975**, *58*, 263.  
 (4) (a) Aten, A. C.; Haanstra, J. H.; deVries, H. *Philips Res. Rep.* **1965**, *20*, 395. (b) Cuthbert, J. D.; Thomas, D. G. *J. Appl. Phys.* **1968**, *39*, 1573. (c) Moulton, P. F. Ph.D. Dissertation, Massachusetts Institute of Technology, 1975.  
 (5) Dutton, D. *Phys. Rev.* **1958**, *112*, 785.  
 (6) Streckert, H. H.; Karas, B. R.; Morano, D. J.; Ellis, A. B. *J. Phys. Chem.* **1980**, *84*, 3232.

(7) (a) Kulp, B. A.; Detweiler, R. M.; Anders, W. A. *Phys. Rev.* **1963**, *131*, 2036 and references therein. (b) Halsted, R. E. In "Physics and Chemistry of II-VI Compounds"; Aven, M., Prener, J. S., Eds.; North-Holland Publishing Co.: Amsterdam, 1967; Chapter 8.

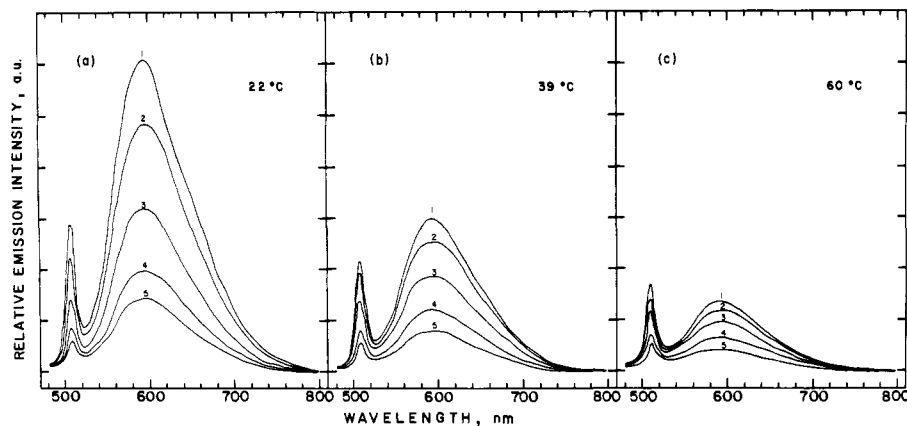


**Figure 1.** Uncorrected emission spectra of a 100-ppm CdS:Te electrode as a function of potential and temperature in sulfide (1 M OH<sup>-</sup>/1 M S<sup>2-</sup>) electrolyte. Frames a, b, and c are data taken at 295, 312, and 333 K, respectively. Curves 1, 2, 3, 4, and 5 in each frame correspond to open circuit, -0.5, -0.3, +0.15 and +0.7 V vs. Ag (PRE), respectively. Pt foil (1 × 3 cm) served as the counterelectrode in the N<sub>2</sub>-purged PEC. Because PEC geometry and incident intensity (~1.7 mW of 457.9-nm excitation incident on the 0.16-cm<sup>2</sup> CdS:Te exposed surface area) were unchanged throughout these experiments, the emissive intensities pictured are directly comparable.

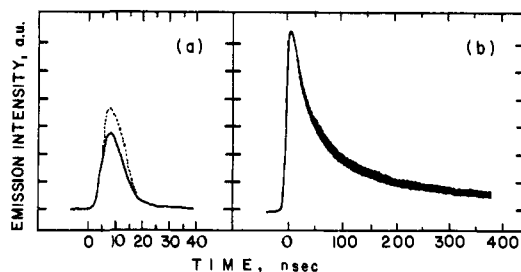


**Figure 2.** Representative intensity-time curves of the 510-nm emission band (a), solid line) and the 600-nm emission band (b). These curves were obtained at 295 K with use of an ~0.16-cm<sup>2</sup>, 100-ppm, single-crystal CdS:Te sample suspended in sulfide electrolyte and excited at 458 nm with a N<sub>2</sub>-pumped dye laser. The intensity-time profile of the excitation source is displayed as the dotted curve in (a). Incident peak power delivered in a typical pulse is estimated to be ~2 kW over an area of ~0.02 cm<sup>2</sup>. Intensities of the three curves are not directly comparable, since they were recorded at different sensitivities.

CdS optical band gap temperature coefficient of  $-5.2 \times 10^{-4}$  eV/K.<sup>8</sup> In contrast, the 600-nm band exhibits a much smaller blue shift in  $\lambda_{\text{max}}$  ( $\leq 10$  nm) in passing from room temperature to 77 K.<sup>2a,9</sup> The 600-nm band has been assigned to a transition involving intraband gap states introduced by the lattice substitution of Te for S; holes trapped in these states, estimated to lie ~0.2 eV above the valence band edge, can recombine with electrons in or near the conduction band to yield the observed emission.<sup>4,9</sup> Scheme I incorporates these assignments into a crude energy diagram in which filled and open circles represent electrons and holes, respectively; the symbols  $E_{\text{CB}}$ ,  $E_{\text{VB}}$ , and  $E_{\text{Te}}$  denote energies of the conduction and valence band edges and of the Te states, respectively. In this scheme the energy of an electron increases in the upward direction, while that of a hole increases in the downward direction.

**2. Decay Times.** Besides their different spectral distributions, another feature which distinguishes the two emission bands is their decay times. Excited-state decay times for the two bands were examined in sulfide medium with use of 458-nm excitation from a N<sub>2</sub>-pumped dye laser. Representative intensity-time curves obtained under these conditions are pictured in Figure 2. The decay profile of the 510-nm band roughly parallels that of the laser pulse (Figure 2a) and indicates that the decay time is <10 ns; no significant change in the decay profile is observed between 295 and 333 K. Although our inability to obtain a more precise value for the 510-nm band is disappointing, we note that a decay time in the nanosecond regime is consistent with the presumed strongly allowed nature of this electronic transition.<sup>10</sup>

The intensity-time curves from which the 600-nm decay time is estimated (illustrated in Figure 2b) have rise times of <10 ns and generally exhibit nonexponential decay; typical  $\tau_{1/e}$  values (measured after a delay of 20 ns from the maximum intensity of the decay profile) at 295 and 333 K are  $120 \pm 40$  and  $80 \pm 30$  ns, respectively. Excitation from electron beams,<sup>4b</sup> a N<sub>2</sub> laser,<sup>9</sup> and  $\alpha$  particles<sup>11</sup> have been reported to give 295-K decay times ( $\tau_{1/e}$ ) as disparate as 1000, 300, and 25 ns, respectively. The discrepancy between our decay times and those in the literature probably reflects the use of different samples and excitation techniques. Our data do accord with results obtained by Richardson, Perone, et al., using samples and excitation conditions more akin to those employed here.<sup>12</sup> Their results also indicate that the 295-K decay time of the 600-nm band is somewhat intensity dependent; from measurements of incident energy per pulse at 458 nm, we estimate that peak powers and intensities of ~2 kW and ~100 kW/cm<sup>2</sup>, respectively, were used in our study.

An important consequence of the inequality in 510- and 600-nm decay times is that it indicates the two excited states are not in thermal equilibrium between 295 and 333 K under the pulse conditions employed.<sup>13</sup> To our knowledge there is no evidence for electron traps at depths comparable to that of the hole trap at  $E_{\text{Te}}$ . Consequently, we attribute lack of thermalization to the holes: hole migration between  $E_{\text{Te}}$  and  $E_{\text{VB}}$  (Scheme I) is not sufficiently rapid relative to  $e^-h^+$  recombination rates to permit the establishment of thermal equilibrium on the time scale of the pulse experiment.

**3. Temperature Effects.** The temperature dependence of the two emission bands is illustrated by the curves labeled "1" in each of Figure 1a, b, and c, corresponding to the open-circuit emission spectra of CdS:Te in sulfide electrolyte at 295, 312, and 333 K, respectively. Only changes in the intensities and not in the spectral distributions of the individual bands are observed over this temperature range. Although both bands lose intensity with increasing temperature, the 600-nm band declines more rapidly. Its intensity falls by a factor of ~4 over the 40° thermal excursion, in agreement with our earlier results.<sup>2c</sup> A comparatively modest 50% decrease in intensity is observed for the 510-nm band. These changes are reversible upon cooling.

Thermal quenching of the 600-nm band of CdS:Te has been ascribed to the activation energy required to promote Te-bound

(10) Pankove, J. I. "Optical Processes in Semiconductors"; Prentice-Hall: Englewood Cliffs, New Jersey, 1971; Chapter 6.

(11) Bateman, J. E.; Ozsan, F. E.; Woods, J.; Cutter, J. R. *J. Phys. D.* **1974**, *7*, 1316.

(12) Richardson, J. H.; Perone, S. P.; Steinmetz, L. L.; Deutscher, S. B. *Chem. Phys. Lett.* **1981**, *77*, 93.

(13) (a) DiBartolo, B. "Optical Interactions in Solids"; Wiley: New York, 1968; Chapter 18.3. (b) Wagner, P. J. In "Creation and Detection of the Excited State", Part A; Lamola, A. A., Ed.; Marcel Dekker: New York, 1971; Vol. I, Chapter 4. (c) Shetlar, M. D. *Mol. Photochem.* **1974**, *6*, 143, 167, 191. (d) Wagner, P. J. *J. Photochem.* **1979**, *10*, 387.

(8) Bube, R. H. *Phys. Rev.* **1954**, *98*, 431.

(9) Roessler, D. M. *J. Appl. Phys.* **1970**, *41*, 4589.

holes back to the valence band.<sup>4,9,11</sup> At the temperatures employed in this study, repopulation of the upper excited state from the lower excited state would be expected for an  $\sim 0.2$  eV energetic separation. Evidence for thermal repopulation at steady state is provided by Figure 1: a semilog plot of the open-circuit intensity ratio (intensity at 510 nm divided by intensity at 600 nm) vs. reciprocal temperature yields a straight line whose slope corresponds to the anticipated activation energy of  $\sim 0.2$  eV.

We had hoped to see back population of the upper excited state reflected in the time-resolved experiments. However, attempts to observe delayed 510-nm emission have thus far been unsuccessful. We ascribe the absence of delayed emission to both the low radiative efficiency of the excited state and the insensitivity of our detection system. Only if the delayed emission intensity had reached a significant fraction ( $\sim 10\%$ ) of the prompt emission intensity would we have detected it.

**4. PEC Properties.** We turn now to the emissive properties of CdS:Te in the context of a PEC. We previously demonstrated that when a CdS:Te photoanode is excited with ultraband gap radiation in a PEC employing polychalcogenide electrolyte, its 600-nm emission band can be quenched by passing photocurrent;<sup>2</sup> in moving to more positive potentials, increased band bending enhances photocurrent by inhibiting  $e^-h^+$  pair recombination.<sup>3</sup>

Curves 1–5 of Figure 1 are the emission spectra observed for the 100-ppm CdS:Te electrode in sulfide electrolyte at increasingly positive bias. The most positive potential of +0.7 V vs. a Ag pseudoreference electrode (PRE) resulted at each temperature in maximum photocurrents of  $\sim 3.1$  mA/cm<sup>2</sup> (a photocurrent quantum efficiency of  $\sim 0.8$ ) and minimum emission intensities. The crucial result is that *at all three temperatures both emission bands are quenched essentially in parallel by passing photocurrent.*

Another presentation of parallel quenching is afforded by Figure 3 which shows the complete current–luminescence–voltage (*iLV*) curve corresponding to Figure 1a. The top portion of Figure 3 was constructed by arbitrarily scaling up the 510-nm emission intensity to match that at 600 nm at open circuit and then scaling up the 510-nm intensity at the other potentials by this same factor. Within experimental error the two curves are congruent. We also found that 476.5-nm excitation yielded very similar results to those presented here using 457.9-nm light.

**5. Mechanistic Implications.** Parallel quenching of multiple emission by passing photocurrent implicates the existence of a mechanism for excited-state communication. Such an interpretation is reinforced by the temperature behavior exhibited in Figure 1: the open-circuit curves demonstrate that at three different temperatures three different sets of excited-state rate constants obtain, yet parallel quenching persists. In this section we examine various excited-state kinetic schemes which are compatible with our data. Key mechanistic points to be considered include the nature of excited-state population, the extent to which the excited states interconvert, their relative contributions to photocurrent, and the effects of potential on the various excited-state decay routes.

We shall call the excited states associated with the 510- and 600-nm emission bands A and B, respectively. Although both states could be populated directly with the ultraband gap excitation employed, we believe that only state A is populated in this manner. Indirect population of B is suggested by the relative absorptivities involved. Absorptivities of impurity-based transitions are typically orders of magnitude less than the  $\sim 10^5$  cm<sup>-1</sup> value observed for band-to-band transitions in CdS and CdS:Te.<sup>4,5,14</sup> We thus favor a scheme wherein A is directly populated and subsequently feeds B. Alternatively, we cannot preclude the existence of a higher energy excited state, C, which could feed A and B. We have, however, no direct evidence for the existence of state C and will subsequently discuss data which argue against its involvement.

The variable-temperature data support the notion that not only is B populated by A, but also interconversion between the states is quite competitive with their other decay processes. Recall that

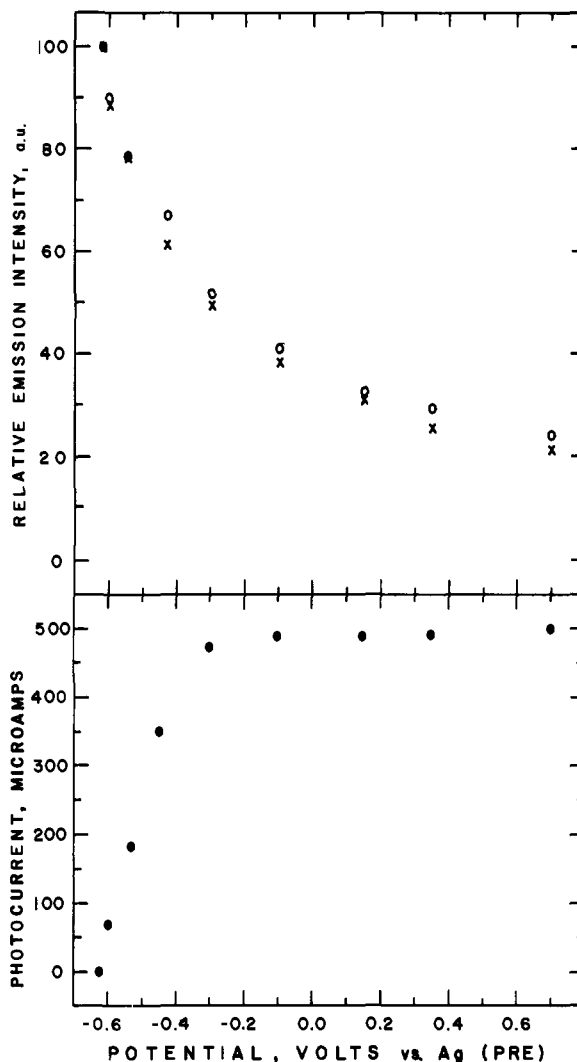


**Figure 3.** Photocurrent (bottom frame) and emission intensity (top frame), monitored at 510 nm (x) and 600 nm (o), vs. electrode potential for the 295-K experiment of Figure 1a. The open-circuit emission intensity at 600 nm has been arbitrarily set at 100 with the 510-nm emission intensity scaled up to match this value. The 510-nm intensity at other potentials was then scaled up by this same factor to obtain the data pictured.

the 510- to 600-nm emission intensity ratio, a measure of the relative populations of A and B, is temperature dependent; a semilog plot of this ratio vs.  $T^{-1}$  is linear with a slope corresponding to the energy gap between the states of  $\sim 0.2$  eV. If not at thermal equilibrium under steady-state conditions, the states appear to be near it.

Quenching for molecular systems possessing multiple excited states has been analyzed in detail.<sup>13b-d</sup> By analogy to molecular systems, parallel quenching of interconverting A and B states will obtain so long as passage of photocurrent does not upset the interconversion of A and B. Disruption of interconversion requires that a considerable fraction of the photocurrent comes from state B. Since we do not observe a significant departure from parallel quenching, we suspect that state A is the principal contributor to photocurrent, i.e., holes are extracted for photocurrent predominantly from  $E_{VB}$  rather than from  $E_{Te}$  (Scheme I). This conclusion is further supported by the similar photocurrent-voltage properties observed with undoped CdS-based PECs for which state B is absent.<sup>2a</sup>

Other schemes which would accommodate parallel quenching include the exoergic feeding of A and/or B by state C with C the contributor of holes to photocurrent. However, the similarity in *iLV* properties obtained with 476.5- and 457.9-nm excitation (vide supra) suggests that the simpler A and B model is more appropriate: energetically, 476.5 nm is sufficiently proximate to the

onset of the 510-nm emission band to effect direct population of state A. We feel that surface states<sup>15</sup> represent a more likely addition to the excited-state manifold than does state C. Although we know little about their role in this system, surface states can influence both excited-state deactivation and charge-transfer processes; their potential effect on the schemes described should be kept in mind.

Implicit in the discussion of quenching has been the assumption that the ratio of radiative to nonradiative recombination efficiency for each of states A and B is unaffected by electrode potential. Relationships observed between emissive and photocurrent quantum efficiencies suggest this to be the case with the particular ratio dependent at least on temperature and excitation wavelength.<sup>26,16</sup> However, Figure 3 demonstrates that potential can influence this ratio: in passing to the most positive potentials, the emission intensity continues to decline while the photocurrent is essentially invariant. Similar effects were observed for n-type, ZnO-based PECs and ascribed to a deficiency in the electron concentration needed for recombination near the surface, a consequence of the large electric field present.<sup>17</sup> In the case of multiple emission, the effect may not be the same for each excited state. For example, we have occasionally seen deviations from parallel quenching at the most positive potentials employed. These results indicate that electrode potential can, in some cases, alter excited-state processes beyond simply serving to divert a fraction of the excited-state population to photocurrent.

The various schemes outlined above are not to be considered exhaustive, but rather as representing what we regard as likely possibilities. In our estimation the most reasonable scheme compatible with our present data consists of direct population of A, interconversion of A and B, and generation of photocurrent principally via state A. Discrimination between this mechanism and several of the alternatives offered may be possible by examining systems with different trap depths and by selective population of the trap-based excited state. Such studies are in progress.

### Experimental Section

**Materials.** Plates of vapor-grown, single-crystal undoped CdS and 100-ppm CdS:Te were obtained from Cleveland Crystals, Inc., Cleveland, Ohio; Te concentration is an estimate based on starting quantities. The  $10 \times 10 \times 1$  mm samples had resistivities of  $\sim 2 \Omega \text{ cm}$  (4 point probe method) and were oriented with their  $10 \times 10$  mm face perpendicular to the *c* axis. Samples were cut into irregularly-shaped pieces  $\sim 0.15 \text{ cm}^2 \times 1$  mm, etched with 1:10 (v/v)  $\text{Br}_2/\text{MeOH}$  for  $\sim 15$  s and subsequently transferred to a beaker of MeOH which was placed in an ultrasonic cleaner to remove residual Br. Etched samples were used either unmounted for decay time studies or mounted as electrodes in a manner previously described.<sup>2a</sup> The preparation of sulfide electrolyte has also been described.<sup>2a</sup>

**Optical Measurements.** Uncorrected emission spectra were obtained with an Aminco-Bowman spectrofluorometer (200–800 nm; bandwidth  $\sim 5$  nm) equipped with a Hamamatsu R446S PMT for extended red response. Spectra were displayed on a HP 7004A X-Y recorder. Sample excitation was achieved by passing the 2–3-mm diameter beam of a Coherent Radiation CR-12 Ar ion laser through a Melles Griot

03-FCG055 long-pass filter (cutoff  $\sim 380$  nm), expanding the beam ten times, and translating it upward via a periscope into a hole in the side of the spectrometer sample compartment. The beam was masked at this point in PEC experiments to fill the electrode surface. Residual exciting light was filtered from the emitted light by placing an aqueous 1 M  $\text{OH}^-/1 \text{ M S}^{2-}/0.2 \text{ M S}$  polysulfide solution in front of the PMT. Laser intensity was measured with a Tektronix J16 radiometer equipped with a J6502 probe head (flat response  $\pm 7\%$ , 450–950 nm). For continuous monitoring of excitation intensity, a quartz disk was used to split part of the beam into a Scientech 362 power meter whose output was recorded on a Heath Model EU-205-11 strip chart recorder. Emission spectra at 77 K were obtained by placing CdS:Te samples in a 21 cm  $\times$  7 mm o.d. tube inserted into a Dewar flask designed to fit into the emission spectrometer chamber. The sample was cooled with liquid  $\text{N}_2$  and the spectrum recorded. Without disturbing the geometry, the liquid  $\text{N}_2$  was allowed to evaporate and the spectrum recorded again after the sample had warmed back to 295 K. Condensation of water on the Dewar flask was prevented by continuously purging the sample compartment with  $\text{N}_2$ .

**Decay Time Measurements.** Samples of CdS:Te were excited with the output of an NRG DL 0.03 dye laser ( $\sim 7$  ns fwhm) which was pumped by an NRG 0.7–5–200 pulsed  $\text{N}_2$  laser (0.7-MW peak power). The detection system consisted of (in series) a Bausch & Lomb Model 33-86-07 monochromator (bandwidth  $\sim 10$  nm), a ferricyanide filter solution (0.06 M  $\text{K}_3\text{Fe}(\text{CN})_6/0.6 \text{ M HCl}$ ; 1.0-cm pathlength cell) to absorb the exciting light, and a Hamamatsu R928 PMT whose base permitted the output to be fed directly into a Tektronix Model 466 storage oscilloscope. Decay curves were obtained by operating the oscilloscope in variable-persistence mode which averaged several hundred pulses. Generally, the laser was run at 20 or 30 pulses/s. A 7.0 cm  $\times$  2.5 cm o.d. Pyrex vessel was used to hold sulfide electrolyte into which the CdS:Te samples, held by Teflon-coated tweezers, were suspended. The sulfide electrolyte was continuously purged by  $\text{N}_2$  via a distilled water reservoir (to maintain solution volume) during the measurements. Samples were positioned at  $\sim 45^\circ$  to both the  $\sim 0.02\text{-cm}^2$  laser beam and the monochromator entrance slit, but the angle was offset slightly to minimize collection of the reflected laser light by the detection optics. Temperature was varied by resistively heating a nichrome wire which surrounded the Pyrex vessel; a calibrated thermometer was used to measure the temperature of the solution. Laser intensity was estimated by accumulating the energy from  $\sim 400$  pulses with the Scientech power meter and correcting for background radiation over the 20-s data collection period.

**PEC Experiments.** A CdS:Te working electrode, a Pt counterelectrode, a Ag pseudoreference electrode (PRE), a magnetic stir bar, and sulfide electrolyte were all placed in the Pyrex vessel which was positioned in the sample compartment of the emission spectrometer. The CdS:Te electrode was oriented at  $\sim 45^\circ$  to both the exciting Ar ion laser beam and the emission detection optics so that principally front-surface emission was detected. A motorized magnet placed beneath the sample chamber was used to stir the electrolyte which was purged by  $\text{N}_2$  and heated as described above. Electrode potential was controlled by a PAR 173 potentiostat/galvanostat with current (PAR 176 I/E converter) displayed on a Varian 9176 strip-chart recorder. Current-luminescence-voltage (*iLV*) curves were taken point-by-point at 295, 312, 333, and 295 K again to demonstrate reproducibility; emission spectra were recorded at each potential as described under Optical Measurements (vide supra). Incident-light intensity was determined by reassembling the PEC outside of the emission spectrometer; the intensity which produced the same *iV* properties was measured with the Tektronix radiometer. Photocurrent in these experiments appeared to be excitation-rate limited, since it varied linearly with light intensity and was not influenced by stirring rate.

**Acknowledgment.** We are grateful to the Office of Naval Research for support of this work. Dr. David Lang of Bell Laboratories and Professor Peter Wagner of Michigan State University are acknowledged for helpful discussions.

(15) Bard, A. J.; Bocarsly, A. B.; Fan, F. F.; Walton, E. G.; Wrighton, M. S. *J. Am. Chem. Soc.* **1980**, *102*, 3671 and references therein.

(16) Ellis, A. B.; Karas, B. R.; Streckert, H. H. *Faraday Discuss. Chem. Soc.*, in press.

(17) Petermann, G.; Tributsch, H.; Bogomolni, R. *J. Chem. Phys.* **1972**, *57*, 1026.